Performance Evaluation of 'Battery-Like' and Hybrid Electrochromic Devices for Dynamic Solar Control in Buildings

Eleftheria Merkoulidi
Department of Physics, Solar Energy Laboratory, University of Patras, Rion, Greece
emerkoulidi@ac.upatras.gr (corresponding author)

George Syrrokostas
Department of Physics, Solar Energy Laboratory, University of Patras, Rion, Greece
gesirrokos@upatras.gr

Received: 16 October 2025 | Revised: 17 December 2025 | Accepted: 29 December 2025

 DOI: https://doi.org/10.48084/etasr.15581

ABSTRACT

This study evaluated the optical and electrochemical properties of tungsten oxide Electrochromic (EC) layers prepared by evaporation and electrodeposition. Minor differences in transparency were observed in the visible part of the solar spectrum. However, evaporated WO_3 films exhibited a charge capacity of 43.75 mC/cm² and a higher bias potential for complete bleaching (approximately 750 mV versus Ag/AgCl). This is in contrast to electrodeposited films, which exhibited a charge capacity of 24.87 mC/cm² and a bias potential of less than 250 mV versus Ag/AgCl. These differences in charge capacity and bias potential are due to the different film morphologies. Film thickness and porosity affect the number of coloration sites and the number of Li^+ ions intercalated into the WO_3 film. Then, "battery-like" and hybrid Electrochromic Devices (h-ECDs) were prepared, achieving a Coloration Efficiency (CE) of up to 52 cm²/C and a contrast ratio of up to 15:1, depending on the device type and EC layer deposition method. Improved open circuit memory was achieved with "battery-like" devices irrespective of the EC layer deposition method. However, hybrid ECDs exhibited lower operating voltages and a lower bleaching capability under short circuit conditions. Thus, h-ECDs consume less energy to change color and are promising alternatives to "battery-like" devices for the dynamic control of incoming solar radiation in buildings.

Keywords-Tungsten oxide; evaporation; electrodeposition; cobalt redox electrolyte; battery-like electrochromic device; hybrid electrochromic device

I. INTRODUCTION

Growth in energy demand in the forthcoming years will be broadly based on three main areas: transport, industry, and buildings. According to a recent report by IEA [1], buildings in Europe account for ~40% of the final energy consumption and ~36% of the Europe's carbon emissions, since heating, cooling, and lighting of buildings require considerable amounts of energy. The same applies also for other places in the world [2]. Currently, only in the European Union, it is estimated that roughly 75% of the building stock is energy inefficient and a vast majority of them will still be in use in 2050 [3]. Therefore, establishment of long-term renovation strategies is important to have achieved zero-emission and fully decarbonized building stock by 2050 [4]. At the same time, more frequent and more intense weather events in the future will lead to an increased impact on buildings' energy performance [5]. Therefore, the energy efficiency improvement in buildings has a key role in meeting global climate goals and ensuring a sustainable built environment.

Of all building components, windows can be regarded as a weak link since they allow considerable heat losses or gains, depending on the difference between the inside and outside temperature, and admit excessive solar irradiation. To rectify this situation, a broad range of heat insulating windows have been developed and are nowadays commercially available [6]. However, seasonal and diurnal variations of weather conditions require dynamic control of the building's thermal load for optimum operation. To this end, smart windows, characterized by their ability to change their appearance in response to an external stimulus, have emerged. Their use may lead to reduced heating and cooling needs and, in some cases, to a reduced demand for lighting [6, 7]. EC windows belong to the class of smart windows, offering dynamic control of their appearance, upon application of a bias potential. The advantages of EC windows and their superior performance have been well documented [8–12]. Hence, one of the key components of an EC window is a thin film that can modulate its optical properties upon reduction or oxidation. Usually, tungsten oxide (WO_3) is used as the EC film exhibits cathodic coloration,

meaning that its coloration takes place due to reduction. It can be deposited as a thin film via various methods, such as vacuum techniques (thermal evaporation, evaporation using an electron beam gun, and sputtering) and chemical techniques (sol–gel deposition, spin–coating, spray pyrolysis, and electrodeposition). Different deposition methods yield films with varying morphologies and coloration efficiencies [13]. In this study, two of the above techniques were used for the fabrication of transparent and uniform WO3 films: evaporation using an electron beam gun and electrodeposition. Optical and electrochemical characterization followed, showing an increased charge capacity in the case of evaporated films, due to differences in the film's morphology. Then, as prepared WO3 films were used in 'battery-like' and in h-ECDs. A liquid electrolyte, based on a LiClO4 salt dissolved in an organic solvent, or an electrolyte containing also cobalt (Co2+) redox active species, was used, respectively. Accordingly, the effect of the different morphologies of the WO3 films on device performance, using the above two electrolytes, was examined, and a more intense effect was found in the case of the redox electrolyte. Finally, the current work constitutes one of the first efforts to use cobalt redox species in an EC device, as other redox couples have already been examined [14].

II. EXPERIMENTAL METHOD

A. Evaporated Tungsten Oxide Films

Thin films of WO_3 were deposited via e-beam gun evaporation on Fluorine doped Tin Oxide (FTO) glass substrates (15 Ω/sq) under high vacuum conditions (P ≈ 10^{-5} mbar) and at room temperature using high-purity (99.99%) WO_3 powder. The film thickness was monitored continuously in situ during deposition using a calibrated quartz crystal sensor and was subsequently verified using an Ambios XP-1 profilometer.

B. Electrodeposited Tungsten Oxide Films

To prepare the peroxytungstate solution, 6.5 g of tungsten powder (99.9% pure) was dissolved in 40 mL of 30% hydrogen peroxide and 4 mL of distilled water. The W powder was added to the H_2O_2 solution progressively under continuous agitation while the solution was inside a chilled water bath. The solution was then stored in a refrigerator at approximately 2 °C for 12 days to allow the W powder to fully dissolve and the excess H_2O_2 to decompose [13]. A portion of the stock solution was mixed with an equal volume of ethanol at room temperature while stirring continuously, yielding a bright yellow liquid [13], which was stored at 2 °C for 3–4 days to ensure optimal deposition results. Before each deposition, the solution was heated at 60 °C for a few min. WO_3 films were electrodeposited using the above solution by applying a 600 mV voltage for 6 min, with current densities of about 1–2 mA/cm² (deposition area: 2.0 × 2.0 cm²), using an Autolab PGSTAT 204 potentiostat/galvanostat. A typical three-electrode configuration was used: a FTO glass sheet (15 Ω/sq) with dimensions of 2.0 cm² x 3.0 cm² as the working electrode; an Ag/AgCl as the reference electrode; and a Pt wire as the counter electrode. The films exhibited a deep blue color during preparation, which vanished almost immediately after removal from the solution. This color change has two aspects: the deep blue color confirms the reduction of tungsten during deposition, and the rapid fading upon voltage removal demonstrates the films' efficient and reversible redox cycling ability, which is a key quality indicator. The films were then rinsed with deionized water and dried with air. Finally, the substrates were heated at 100 °C for 1 h.

C. Optical and Electrochemical Characterization of WO_3 Films

Optical characterization was conducted, using a PerkinElmer Lambda 650 UV/Vis spectrometer. Specifically, transmittance $T(\lambda)$ spectra in the visible spectrum were recorded at normal incidence. Then, the luminous transmittance T_{lum} was calculated:

$$T_{lum} = \frac{\int_{400\ nm}^{680\ nm} f(\lambda)\, T(\lambda)\, d\lambda}{\int_{400\ nm}^{680\ nm} f(\lambda)\, d\lambda} \quad (1)$$

where $f(\lambda)$ is the sensitivity of the human eye in the photopic state. Cyclic voltammetry experiments were carried out using the above electrochemical setup to assess the electrochemical properties of the films. The electrolyte was 1 M $LiClO_4$ in Propylene Carbonate (PC), and the applied potential window was from −1.0 V to +0.8 V with a scan rate of 50 mV/s. Cyclic voltammetry is used, among other things, to calculate the total charge density of Li^+ ions intercalated and deintercalated into the films. The charge density was calculated:

$$Q\ (t) = \int J(t)\, dt \quad (2)$$

where Q (mC/cm^2) and J (mA/cm^2) are the charge density and the current density, respectively.

D. Fabrication of EC Devices

- Battery-like EC devices: The as-prepared WO_3 electrodes were used in battery-like EC devices with the structure, FTO/WO_3/1 M $LiClO_4$-PC/FTO. Two small holes were drilled in the second FTO glass substrate to serve as the cathode and facilitate pouring the electrolyte into the EC device. The two electrodes were arranged facing each other, slightly displaced to preserve space for the electrical contacts. The device was sealed using a 0.5 mm thermoplastic material (PV5414) at 120 °C for a few min under pressure, which also acted as a spacer. Three pieces of the thermoplastic material were used to ensure the desired spacing between the electrodes. The space between the electrodes was filled by pouring the liquid electrolyte through one hole while expelling the air through the other. Finally, the holes were sealed with small pieces of glass and thermoplastic material (Surlyn, 50 μm thick, from Greatcellsolar).
- Hybrid EC devices: In this case, WO_3 electrodes were used in hybrid EC devices with the structure, FTO/WO_3/redox electrolyte/Pt/FTO. The platinized FTO glass substrate served as the cathode and was prepared by electrodeposition [14]. The devices were arranged as in the case of battery-like devices, but with different thermoplastic materials used to control the distance between the two electrodes. Finally, the space between the two electrodes was filled with a liquid redox electrolyte composed of 0.22 M Co(II)PF6 (FK 102, supplied by Greatcell Solar), 0.5 M

LiClO4, and 0.5 M 4-TBP in an equivolumetric solution of acetonitrile and 3-methoxypropionitrile [15], as in the case of battery-like devices.

E. Optical Characterization of EC Devices

The devices were colored at a constant current of 0.2 mA (galvanostatically) for various time intervals. Thus, a certain amount of electric charge was gradually fed into the devices. Transmittance ($T(\lambda)$) spectra were recorded at normal incidence during different coloration stages, and CE was calculated at 630 nm, which is a key performance metric for ECDs because it quantifies the degree of optical modulation achieved per unit of charge exchanged. CE is defined as the ratio of the change in optical density (ΔOD) to the intercalated charge density (Q), expressed in C/cm², where ΔOD is obtained from the logarithmic ratio of the transmittance in the bleached and colored states of the device:

$$\Delta OD = log\left[\frac{T_{bleached}(\lambda)}{T_{colored}(\lambda)}\right] \quad (3)$$

$$CE\ (\lambda) = \frac{\Delta OD\ (\lambda)}{Q} \quad (4)$$

where CE is expressed in units of cm^2/C and is wavelength-dependent, with its value varying according to the specific wavelength at which the measurement is performed.

III. RESULTS AND DISCUSSION

A. Tungsten Oxide Films

Figure 1 shows the transmittance spectra of the WO_3 films prepared using the two methods and compared to a bare FTO glass substrate. In both cases, the WO_3 films are highly transparent in the visible spectrum without significantly affecting the transparency of the bare FTO glass substrate.

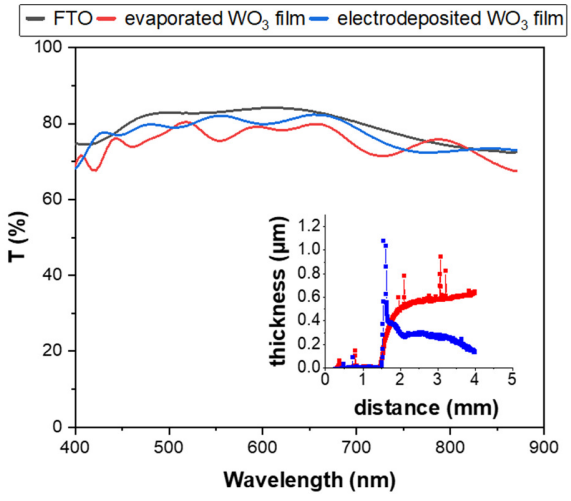

Fig. 1. Transmittance spectra of a bare FTO glass substrate and after depositing WO_3 thin films by the two methods:evaporation, electrodeposition (inset: thickness profile of WO_3 thin films).

More specifically, the T_{lum} values were 77.1% and 80.7% for an evaporated and an electrodeposited film, respectively, compared to 83.2% for a bare FTO glass substrate. The slight difference in T_{lum} values between the WO_3 films is due to their different thicknesses; the typical thickness of evaporated WO_3 films is 550 nm, while that of electrodeposited films is approximately 350 nm. The surface roughness is comparable in both cases (approximately 30 nm), ruling out the presence of surface conglomerates for electrodeposited films [13]. The cyclic voltammograms of WO_3 films are presented in Figure 2, and their shape is typical of amorphous films [16–18]. A significant difference in the areas of the two voltammograms was observed, which is proportional to the total charge density of Li^+ ions intercalated and deintercalated into the films, or equally/equal to the films' charge storage capacity [19]. Consequently, the total charge density was 43.75 mC/cm² and 24.87 mC/cm² for the evaporated and electrodeposited WO_3 films, respectively. Similarly, the coloration current at the most negative value on the CV plot is nearly one and a half times higher for the evaporated film than for the electrodeposited film.

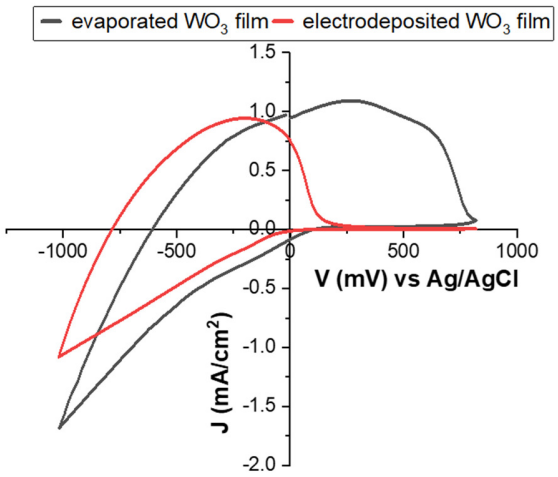

Fig. 2. Typical cyclic voltammograms of as-prepared WO_3 thin films, deposited by the two methods: evaporation, electrodeposition.

Two further characteristic points in the case of electrodeposited WO_3 films, compared to evaporated films, are complete bleaching at a lower bias potential, showing that de-intercalation of Li^+ ions is easier, and a minor negative shift of the voltage value where coloration begins. The above results can be explained by different film morphologies, including film thickness and porosity [20–22]. As film thickness increases, more colored sites exist, expecting to see increased values in the overall voltammogram area, as well as increased charge capacity. Complete bleaching at a higher bias potential is also expected to be seen. On the other hand, a film with a more open structure could increase the mobility of Li^+ ions. To evaluate stability, 100 consecutive coloration-bleaching cycles were performed, as depicted in Figure 3. No significant changes were observed in the case of an evaporated WO_3 film apart from the progressive reduction of the positive bias potential for complete bleaching of the film, especially during the first 50 cycles (from nearly 700 mV to less than 550 mV). Improved wetting of the films by the electrolyte during cycling

offers more entry and exit points for Li^+, thus simplifying the extraction of Li^+ ions. However, the above training phenomenon was not observed in the case of an electrodeposited WO_3 film due to its more open structure, which permits complete wetting by the electrolyte. Overall, the films presented in this study are stable and insensitive to continuous cycling.

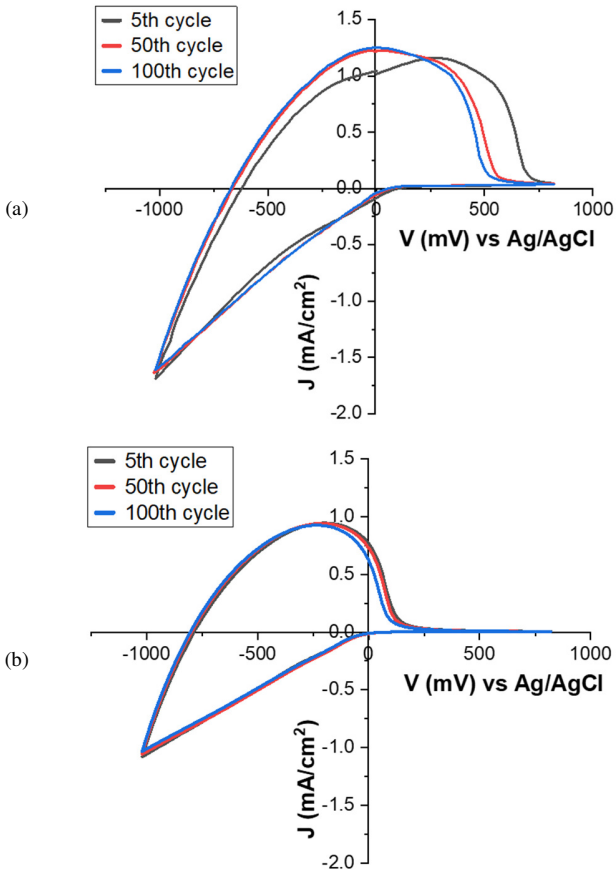

Fig. 3. Representative CV curves of WO_3 thin films deposited by the two methods: (a) evaporation and (b) electrodeposition for the 5th, 50th, and 100th cycles.

B. 'Battery-Like' Electrochromic Devices

As-prepared evaporated and electrodeposited WO_3 films were used to fabricate battery-like ECDs. Figures 4 (a) and 4 (b) display the transmittance spectra of an ECD with an evaporated WO_3 film and an ECD with an electrodeposited film at various coloration stages, respectively. Both devices are highly transparent in the visible part of the spectrum when bleached, and they exhibit rapid coloration during the initial stages, especially in the near-infrared part of the spectrum. However, the device with the evaporated WO_3 film exhibited improved coloration depth compared with the electrodeposited film, due to its higher thickness, which resulted in a greater number of coloration sites. The improved coloration depth, as shown by the calculated T_{lum} values in both cases, was achieved despite nearly the same charge density being fed into the devices. Therefore, a higher CE is expected for the evaporated films. A higher CE value indicates that significant optical contrast can be achieved with minimal charge consumption, a feature directly linked to a faster switching response.

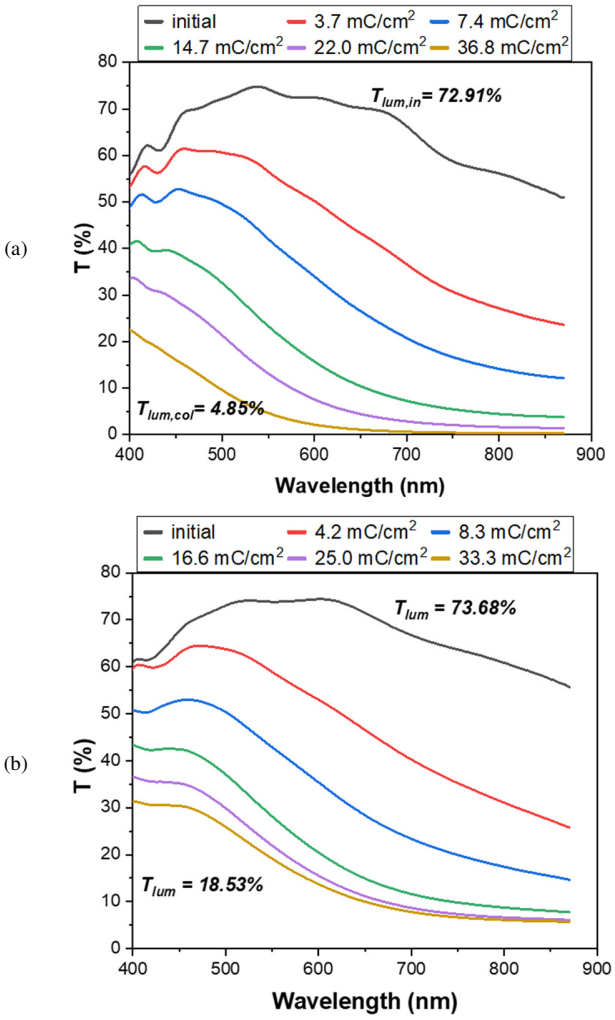

Fig. 4. Transmittance spectra of 'battery-like' ECDs having: (a) an evaporated WO_3 thin film and (b) an electrodeposited WO_3 thin film, at different steps of inserted charge.

Figure 5 illustrates the variation of optical density with respect to charge density. Evaporated films exhibited a greater change in optical density for the same amount of intercalated charge compared to electrodeposited films. Consequently, the CE was 52 cm²/C for evaporated WO_3 films and 42.6 cm²/C for electrodeposited films at 630 nm. Another critical parameter is the ability of the devices to retain their color state without a continuous bias potential. This is an open-circuit memory, where the devices were colored by applying a constant bias potential of -3 V for 3 min, after which they were left in open-circuit conditions. Figure 6 presents the transparency at 600 nm and the potential difference across the terminals. After 5 min at open circuit conditions, no significant changes in the transparency of the devices were observed. However, a notable

decrease in potential across the terminals of the devices was evidenced. Specifically, after 5 min at open-circuit conditions, the potential decreased from 3 V to 1.7 V and 1.5 V for the evaporated and electrodeposited WO_3 films, respectively.

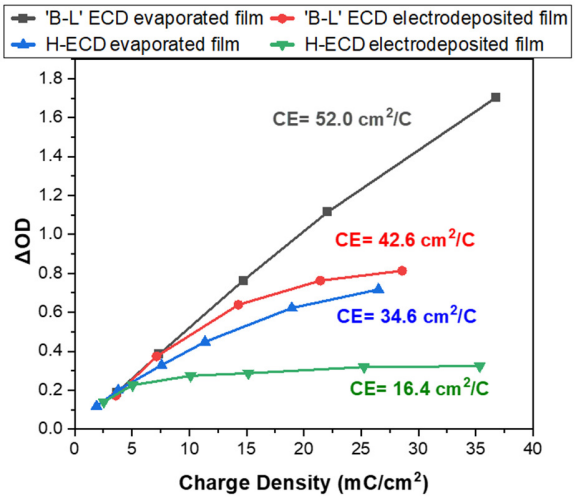

Fig. 5. Variation in the optical density (ΔOD) in respect with the charge density at 630 nm for 'battery-like' ($LiClO_4$) and hybrid (Co^{+2}/Co^{+3}) ECDs, having both evaporated and electrodeposited WO_3 thin films.

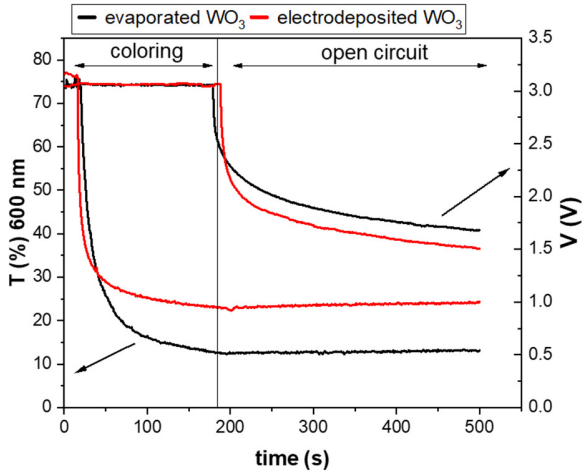

Fig. 6. Variation in the transmittance and in the potential difference across the terminals of 'battery-like' ECDs, having both evaporated and electrodeposited WO_3 thin films, during coloration and at open circuit conditions.

Although self-bleaching did not occur, significant self-discharging showed that the devices cannot be considered EC batteries. However, they can be used as smart windows due to their intense optical modulation, especially in the infrared spectrum. In other words, the devices can retain their optical state but not the potential difference across their terminals.

C. Hybrid Electrochromic Devices

Hybrid EC devices also used evaporated and electrodeposited WO_3 films as-prepared. In this case, a cobalt-based redox electrolyte was utilized. Due to the electrolyte's absorption in the visible part of the spectrum [15], the distance between the two electrodes had to be optimized to ensure high transparency. Initially, one piece of a 500-μm-thick thermoplastic material (PV5414) was used. As shown in Figure 7, intense absorption was observed for wavelengths up to 550 nm, rendering the device unsuitable for use as a smart window. To reduce the distance between the two electrodes, three 150-μm-thick pieces of Surlyn, another thermoplastic material, were used. As a result, absorption in the visible spectrum decreased, and the devices still had a pale yellowish tint, showing that further efforts to optimize the distance or the optical properties of the electrolyte are needed.

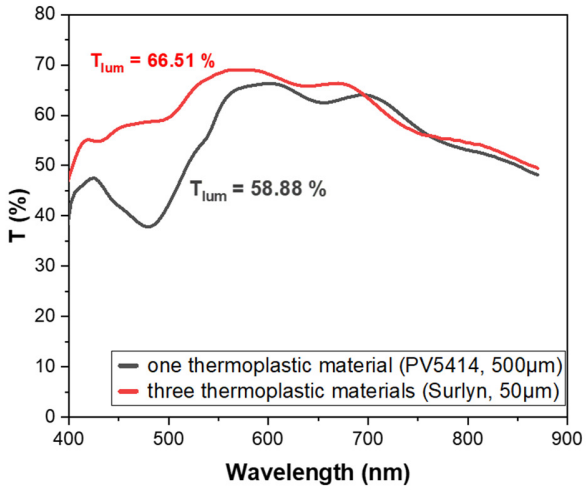

Fig. 7. Initial transmittance spectra of a hybrid ECD having different distance between the electrodes.

Figures 8 (a) and 8 (b) present the transmittance spectra of hybrid EC devices with various cumulative intercalated charge densities. One uses an evaporated WO_3 film, and the other uses an electrodeposited film. From the initial stages of coloration, intense coloration is evident only in the case of the evaporated film. Consequently, the T_{lum} value varied from 66.5% to 21% for the evaporated film and from 66.6% to 40% for the electrodeposited film, despite the use of a lower charge density. As expected, the CE decreased from nearly 35 to 16 cm²/C at 630 nm due to the greater change in optical density for the same amount of intercalated charge in the evaporated WO_3 films. However, the optical modulation in the visible spectrum was inferior to that of battery-like devices, even with a higher current applied (0.4 mA). Due to direct contact with the EC layer, a loss current appears when the redox species are present, which negatively affects the color depth and open-circuit memory of h-ECDs. Authors in [23-28] propose various methods to address this self-bleaching mechanism. Moreover, significant optical losses occur due to self-bleaching at open circuit conditions for both devices. Consequently, the transmittance of the devices at 600 nm increased from 20% to 31% and from 25% to 42% for the evaporated and electrodeposited WO_3 films, respectively, after only 3 min at open-circuit conditions, as portrayed in Figure 9. Electrodeposited films with a more open structure have a greater interface area with the electrolyte. This promotes the

reduction of cobalt species, and thus self-bleaching. Coloration occurred when applying a bias potential of 1.5 V for 2 min instead of 3 V for 3 min, as in the case of battery-like ECDs. Therefore, hybrid devices can exhibit a lower operating voltage.

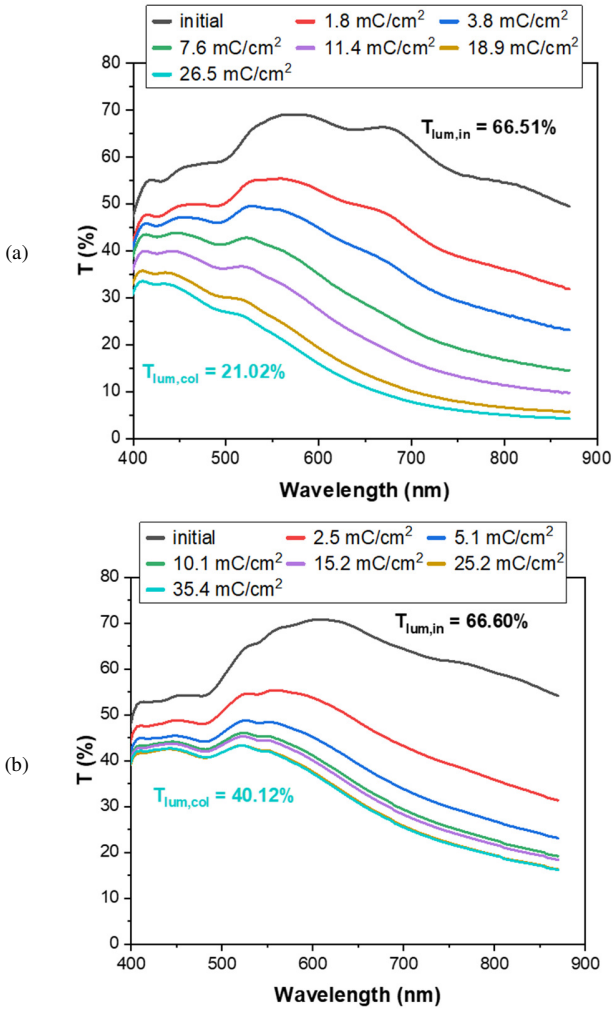

Fig. 8. Transmittance spectra of h-ECDs having: (a) an evaporated WO_3 thin film and (b) an electrodeposited WO_3 thin film, at different steps of inserted charge.

Finally, complete bleaching of the devices can occur at short-circuit conditions, as shown in Figure 10, without reversing the polarity of the bias potential. This means that no energy is consumed during bleaching, unlike battery-like ECDs, which improves their energy-saving potential further. Currently, there are no large-scale applications of h-ECDs; therefore, the effect of device area on switching time is still unknown. In contrast, the response time of battery-like devices is slower as the device area increases.

IV. CONCLUSIONS

In this study, high-quality WO_3 thin films were deposited on Fluorine doped Tin Oxide (FTO) glass surfaces through evaporation and electrodeposition. The films exhibited similar luminous transmittance values (78-80%). The evaporated WO_3 films exhibited an improved charge capacity of 43.75 mC/cm², due to their higher film thickness compared to the electrodeposited films (24.87 mC/cm²).

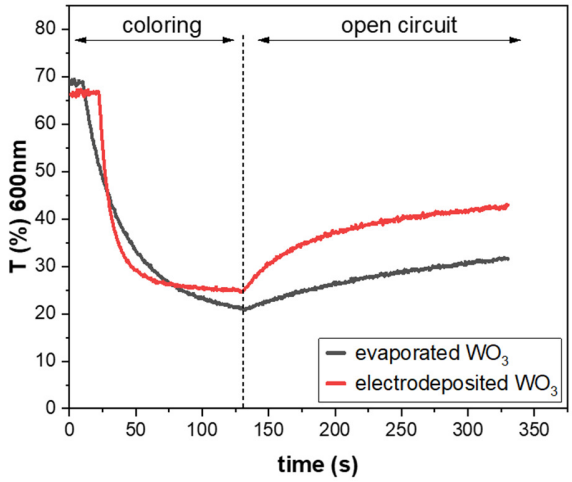

Fig. 9. Variation in the transmittance of h-ECDs, having both evaporated and electrodeposited WO_3 thin films, during coloration and at open circuit conditions.

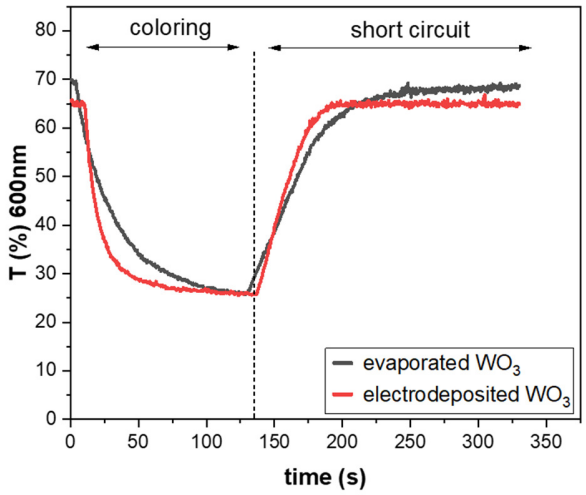

Fig. 10. Variation in the transmittance of h-ECDs, having both evaporated and electrodeposited WO3 thin films, during coloration and at open circuit conditions.

A training period was necessary to create more entry/exit points for Li^+ during continuous coloration-bleaching cycles. On the other hand, the electrodeposited films exhibited improved stability up to 100 consecutive cycles and complete bleaching at a lower bias potential. This was attributed to the films' different thicknesses and open structures. Then, the WO_3 films, both evaporated and electrodeposited, were used as the Electrochromic (EC) layer in battery-like and hybrid Electrochromic Devices (h-ECDs). The contrast ratio and Coloration Efficiency (CE) of battery-like devices with an evaporated WO_3 film were 15:1 and 52 cm²/C, respectively,

compared to 4:1 and 42.6 cm²/C for a similar device with an electrodeposited WO_3 film. These results are consistent with the improved charge capacity of the evaporated films. Additionally, the open circuit memory of the devices was excellent, exhibiting minimal optical loss after 5 min under open circuit conditions, regardless of the film preparation method. However, self-discharging was observed, wherein the potential difference across the terminals of the devices decreased. Self-discharging is rarely reported in the literature and requires further examination to fully exploit the advantages of ECDs as smart windows for dynamically controlling solar light entering buildings and as EC batteries and supercapacitors. In the last two cases especially, minimizing electrical losses is crucial and could be a key area for future mechanistic investigation in the field of EC charge-storing devices. Finally, h-ECDs with a cobalt-based redox electrolyte exhibited an initial yellowish tint, even when the distance between the two electrodes was reduced from 500 μm to 150 μm. Due to self-bleaching, the contrast ratio and CE of hybrid devices with an evaporated WO_3 film were 3:1 and 34.6 cm²/C, respectively, compared to 1.7:1 and 16.4 cm²/C for a similar device with an electrodeposited WO_3 film. Direct comparison of the two device types revealed that battery-like devices outperformed h-ECDs, contrary to what is usually reported in the literature. This highlights the need to optimize the properties of the cobalt redox electrolyte. Nevertheless, lower operating voltages and bleaching under short-circuit conditions explain why h-ECDs with a cobalt-based redox electrolyte are worth developing. Self-bleaching was more intense for electrodeposited films due to their open structure, which creates a larger interfacial area between WO_3 and the electrolyte, leading to considerable optical losses. The present study confirms that the morphology of the EC layer depends on the deposition method. Consecutive cycling creates more ion/electron pathways in evaporated films, improving the optical and charge storage properties of ECDs. In electrodeposited films, a more open structure creates a high reaction surface area, decreasing coloration time and enhancing self-bleaching in h-ECDs.

ACKNOWLEDGMENT

The authors acknowledge financial support from the project ‘FENESTRAE’ co-funded by the European Union through the Interreg IPA ADRION program. This paper has been produced with the financial assistance of the European Union. The content of the document is the sole responsibility of University of Patras, Department of Physics, and cannot, under any circumstances, be regarded as reflecting the position of the European Union and/or IPA ADRION program authorities.

REFERENCES

[1] G. Eder *et al.*, *Coloured BIPV: Market, Research and Development*, IEA PVPS Task 15, Subtask E, Report IEA-PVPS T15-07:2019, International Energy Agency, Feb. 2019

[2] F. A. AlFaraidy and S. Azzam, "Residential Buildings Thermal Performance to Comply With the Energy Conservation Code of Saudi Arabia," *Engineering, Technology & Applied Science Research*, vol. 9, pp. 3949–3954, 2019, https://doi.org/10.48084/etasr.2536.

[3] Energy Performance of Buildings Directive. European Commission, 2025.

[4] G. Sut, B. B. Colak Demirel, and F. Goksen Takva, "Renovation Strategies for Energy Conservation in Multi-Story Residential Buildings in Turkey," *Engineering, Technology & Applied Science Research*, vol. 14, pp. 16135–16141, 2024, https://doi.org/10.48084/etasr.7962.

[5] K. G. Droutsa, S. Kontoyiannidis, C. A. Balaras, A. A. Argiriou, E. G. Dascalaki, K. V. Varotsos, and C. Giannakopoulos, "Climate Change Scenarios and Their Implications on the Energy Performance of Hellenic Non-Residential Buildings," *Sustainability*, vol. 13, no. 23, 2021, Art. no. 13005, https://doi.org/10.3390/su132313005.

[6] R. Baetens, B. P. Jelle, and A. Gustavsen, "Properties, requirements and possibilities of smart windows for dynamic daylight and solar energy control in buildings: A state-of-the-art review," *Solar Energy Materials and Solar Cells*, vol. 94, pp. 87–105, 2010, https://doi.org/10.1016/j.solmat.2009.08.021.

[7] L. L. Fernandes, E. S. Lee, and G. Ward, "Lighting energy savings potential of split-pane electrochromic windows controlled for daylighting with visual comfort," *Energy and Buildings*, vol. 61, pp. 8–20, 2013, https://doi.org/10.1016/j.enbuild.2012.10.057.

[8] C. G. Granqvist, "Electrochromics for smart windows: Oxide-based thin films and devices," *Thin Solid Films*, vol. 564, pp. 1–38, 2014, https://doi.org/10.1016/j.tsf.2014.02.002.

[9] A. Aldawoud, "Conventional fixed shading devices in comparison to an electrochromic glazing system in hot, dry climate," *Energy and Buildings*, vol. 59, pp. 104–110, 2013, https://doi.org/10.1016/j.enbuild.2012.12.031.

[10] S. H. N. Lim, J. Isidorsson, L. Sun, B. L. Kwak, and A. Anders, "Modeling of optical and energy performance of tungsten-oxide-based electrochromic windows including their intermediate states," *Solar Energy Materials and Solar Cells*, vol. 108, pp. 129–135, 2013, https://doi.org/10.1016/j.solmat.2012.09.010.

[11] N. DeForest, A. Shehabi, G. Garcia, J. Greenblatt, E. Masanet, E. S. Lee, S. Selkowitz, and D. J. Milliron, "Regional performance targets for transparent near-infrared switching electrochromic window glazings," *Building and Environment*, vol. 61, pp. 160–168, 2013, https://doi.org/10.1016/j.buildenv.2012.12.004.

[12] J. Mardaljevic and A. Nabil, "Electrochromic glazing and facade photovoltaic panels: a strategic assessment of the potential energy benefits," *Lighting Research & Technology*, vol. 40, pp. 55–76, 2008, https://doi.org/10.1177/1477153507083906.

[13] M. Giannouli and G. Leftheriotis, "The effect of precursor aging on the morphology and electrochromic performance of electrodeposited tungsten oxide films," *Solar Energy Materials and Solar Cells*, vol. 95, no. 7, pp. 1932–1939, July 2011, https://doi.org/10.1016/j.solmat.2011.02.024.

[14] G. Syrrokostas, S. Tsamoglou, and G. Leftheriotis, "Limitations Imposed Using an Iodide/Triiodide Redox Couple in Solar-Powered Electrochromic Devices," *Energies*, vol. 16, no. 20, p. 7084, Jan. 2023, https://doi.org/10.3390/en16207084.

[15] A. Dokouzis, D. Zoi, and G. Leftheriotis, "Photoelectrochromic devices with enhanced power conversion efficiency," *Materials*, vol. 13, no. 11, 2020, Art. no. 2565, https://doi.org/10.3390/ma13112565.

[16] C. O. Avellaneda, P. R. Bueno, R. C. Faria, and L. O. S. Bulhões, "Electrochromic properties of lithium doped WO3 films prepared by the sol–gel process," *Electrochimica Acta*, vol. 46, nos. 13–14, pp. 1977–1981, 2001, https://doi.org/10.1016/S0013-4686(01)00372-3.

[17] P. R. Bueno, C. O. Avellaneda, R. C. Faria, and L. O. S. Bulhões, "Electrochromic properties of undoped and lithium doped Nb2O5 films prepared by the sol–gel method," *Electrochimica Acta*, vol. 46, nos. 13–14, pp. 2113–2118, 2001, https://doi.org/10.1016/S0013-4686(01)00381-4.

[18] C. G. Granqvist, *Handbook of Inorganic Electrochromic Materials*, Elsevier, Amsterdam, The Netherlands, 2002

[19] G. Leftheriotis, S. Papaefthimiou, P. Yianoulis, A. Siokou, and D. Kefalas, "Structural and electrochemical properties of opaque sol–gel deposited WO3 layers," *Applied Surface Science*, vol. 218, pp. 276–281, 2003, https://doi.org/10.1016/S0169-4332(03)00616-0.

[20] M. H. Kim, H. W. Choi, and K. H. Kim, "Thickness Dependence of WO3 Thin Films for Electrochromic Device Application," *Molecular*

Crystals and Liquid Crystals, vol. 598, pp. 54–61, 2014, https://doi.org/10.1080/15421406.2014.933298.

[21] B. Wen-Cheun Au, K.-Y. Chan, and D. Knipp, "Effect of film thickness on electrochromic performance of sol–gel deposited tungsten oxide (WO3)," *Optical Materials*, vol. 94, pp. 387–392, 2019, https://doi.org/10.1016/j.optmat.2019.05.051.

[22] S. S. Kalagi, S. S. Mali, D. S. Dalavi, A. I. Inamdar, H. Im, and P. S. Patil, "Transmission attenuation and chromic contrast characterization of R.F. sputtered WO3 thin films for electrochromic device applications," *Electrochimica Acta*, vol. 85, pp. 501–508, 2012, https://doi.org/10.1016/j.electacta.2012.08.093.

[23] J. Bae, H. Kim, H. C. Moon, and S. H. Kim, "Low-voltage, simple WO3-based electrochromic devices by directly incorporating an anodic species into the electrolyte," *Journal of Materials Chemistry C*, vol. 4, pp. 10887–10892, 2016, https://doi.org/10.1039/C6TC03463B.

[24] S. Bogati, A. Georg, C. Jerg, and W. Graf, "Tetramethylthiourea (TMTU) as an alternative redox mediator for electrochromic devices," *Solar Energy Materials and Solar Cells*, vol. 157, pp. 454–461, 2016, https://doi.org/10.1016/j.solmat.2016.07.023.

[25] M. Čolović, M. Hajzeri, M. Tramšek, B. Orel, and A. K. Surca, "In situ Raman and UV–visible study of hybrid electrochromic devices with bis end-capped designed trialkoxysilyl-functionalized ionic liquid based electrolytes," *Solar Energy Materials and Solar Cells*, vol. 220, 2021, Art. no. 110863, https://doi.org/10.1016/j.solmat.2020.110863.

[26] K. Sheng, F. Xu, K. Shen, J. Zheng, and C. Xu, "Electrocatalytic PProDOT–Me2 counter electrode for a Br−/Br3− redox couple in a WO3-based electrochromic device," *Electrochemistry Communications*, vol. 111, 2020, Art. no. 106646, https://doi.org/10.1016/j.elecom.2019.106646.

[27] R. Giannuzzi, C. T. Prontera, V. Primiceri, A. L. Capodilupo, M. Pugliese, F. Mariano, A. Maggiore, G. Gigli, V. Maiorano, "Hybrid electrochromic device with transparent electrolyte," *Solar Energy Materials and Solar Cells*, vol. 257, 2023, Art. no. 112346, https://doi.org/10.1016/j.solmat.2023.112346.

[28] J. Song, B. Huang, Y. Xu, K. Yang, Y. Li, Y. Mu, L. Du, S. Yun, L. Kang, "A Low Driving-Voltage Hybrid-Electrolyte Electrochromic Window with Only Ferreous Redox Couples," *Nanomaterials*, vol. 13, no. 1, 2023, Art. no. 213, https://doi.org/10.3390/nano13010213.